VIP Solar Cells Very Important Paper

Deutsche Ausgabe: DOI: 10.1002/ange.201503933
Internationale Ausgabe: DOI: 10.1002/anie.201503933

# Finely Tuned Polymer Interlayers Enhance Solar Cell Efficiency

*Yao Liu, Zachariah A. Page, Thomas P. Russell,* and Todd Emrick**

***Abstract:*** *Three conjugated polymer zwitterions (CPZs), containing thiophene-, diketopyrrolopyrrole- (DPP), and naphthalene diimide (NDI) backbones, were synthesized with pendant zwitterions, specifically sulfobetaine groups. Diboronate-ester-functionalized bithiophene and benzothiadiazole monomers were copolymerized with zwitterion-substituted dibromothiophene, DPP, and NDI monomers by $A_2+B_2$ Suzuki polymerization. The CPZs were incorporated into polymer solar cells (PSCs) as interlayers between the photoactive layer and Ag cathode. The thiophene-based CPZs gave power conversion efficiencies (PCEs) of about 5 %, while the narrow-energy-gap DPP- and NDI-based CPZs performed exceptionally well, giving PCEs of 9.49 % and 10.19 %, respectively. The interlayer thickness had only a minor impact on the device performance for the DPP- and NDI-CPZs, a finding attributed to their electron-transport properties. Ultraviolet photoelectron and reflectance spectroscopies, combined with external quantum efficiency measurements, provided structure–property relationships that lend insight into the function of CPZ interlayers in PSCs. NDI-based CPZ interlayers provide some of the best performing organic solar cells reported to date, and prove useful in conjunction with high-performing polymer-active layers and stable, high-work-function, metal cathodes.*

Polymer solar cells (PSCs) provide an avenue to inexpensive renewable energy by large-scale printing of lightweight and flexible materials. PSCs are typically composed of multiple layers, where electronic communication at each interface is crucial for achieving high efficiency. As such, interfacial engineering is needed to enhance device performance.[1,2] For example, interlayers located between the active layer and conductive electrodes improve the selectivity of charge transport, and minimize series resistance ($R_s$), leading to PCE values exceeding 9 % for single junction PSCs.[3–7] A blend of poly(ethylenedioxythiophene) and poly(styrene sulfonate) (PEDOT:PSS) functions as a solution-processible hole-selective anode modification layer that has proven generally useful for PSCs. Recent efforts have been devoted to developing new cathode modification layers to enhance electron extraction efficiency. Small-molecule organic interlayers integrated into PSCs afford noteworthy device improvement, including functional fullerenes,[4,8–16] perylene diimides,[17] and oligomeric fluorenes.[5] Polymer interlayers provide advantages of both facile solution processing and robust film formation, with two recently reported examples being poly(ethyleneimine) (PEI)[18,19] and tertiary-amine-substituted polyfluorene (PFN).[3,20]

Cathode modification layers that impart a negative interfacial dipole ($\Delta$) lower the electrode work function and increase the electrostatic potential across the device.[21] This in turn enables the use of stable, high-work-function metals in devices, while the enhanced E-field increases the generation of free charges and extraction efficiency, maximizing short-circuit current density ($J_{SC}$) and fill factor (*FF*). The interfacial dipole increases the anode–cathode work function offset ($\Phi_{A-C}$), thus enhancing open circuit voltage ($V_{OC}$).[22] Polar semiconducting polymers, such as conjugated polyelectrolytes (CPEs)[23–25] and conjugated polymer zwitterions (CPZs),[26–29] provide large negative $\Delta$ values to metals, with an inherent tunability of electronic properties. We designed novel CPZs as neutral, electronically active, hydrophilic semiconducting polymers, having two pendant sulfobetaine groups per repeat unit. Such polymers promise to overcome the general shortcoming in most cathode modification layers (i.e., having aliphatic or *p*-type backbones) of inefficient electron transport that requires interlayers to be very thin (about 5 nm or less). To circumvent this, new interlayers with appreciable electron-transport properties are needed to reduce the deleterious impact of charge build-up and surface recombination in devices.

An ideal cathode modification layer would lower the electrode work function ($\Phi$), have solubility properties orthogonal to those of the photoactive layer, exhibit good film-forming properties (wettability/uniformity), transport electrons selectivity, possess large electron affinity ($E_A$), and exhibit long-term stability. No current interlayers satisfy all of these requirements, but understanding their structure–property relationships will enable the rational design of optimized new materials. Here we report the synthesis and characterization of CPZs for organic photovoltaics (OPVs), and demonstrate how transport properties of CPZ interlayers influence solar-cell performance.

Our synthesis of sulfobetaine (SB)-functionalized thiophene, diketopyrrolopyrrole (DPP), and naphthalene diimide (NDI) monomers hinged on incorporating tertiary amines into the aromatic monomer precursors for ring-opening of 1,3-propanesultone (detailed procedures in the Supporting Information). As shown in Figure 1, CPZs were obtained by Suzuki–Miyaura (S-M) coupling/polymerization of dibrominated SB monomers with diboronate ester bithiophene to give poly(trithiophene sulfobetaine) (**$PT_3SB$**), and poly(bithiophene naphthalene diimide sulfobetaine) (**$PT_2NDISB$**), as well as with diboronate-ester benzothiadiazole to afford

[*] Dr. Y. Liu,[+] Z. A. Page,[+] Prof. Dr. T. P. Russell, Prof. Dr. T. Emrick
Polymer Science and Engineering Department
University of Massachusetts Amherst
120 Governors Drive, Amherst, MA 01003 (USA)
E-mail: russell@mail.pse.umass.edu
tsemrick@mail.pse.umass.edu

[+] These authors contributed equally to this work.

Supporting information for this article is available on the WWW under http://dx.doi.org/10.1002/anie.201503933.

  

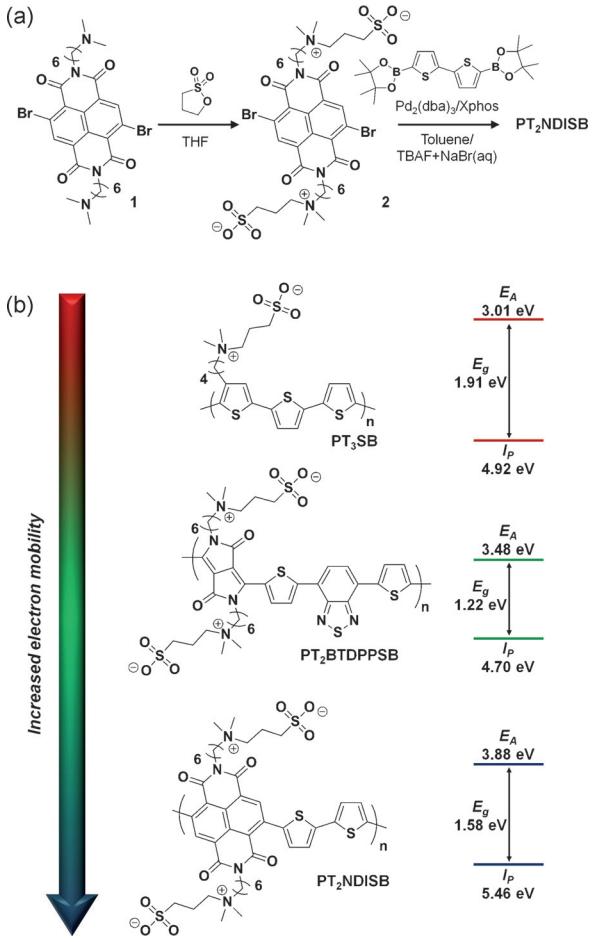


***Figure 1.*** a) Synthesis of **$PT_2$NDISB**. b) Chemical structures and experimentally determined energy levels for **$PT_3$SB**, **$PT_2$BTDPPSB**, and **$PT_2$NDISB**.

poly(bithiophene-benzothiadiazole diketopyrrolopyrrole-sulfobetaine) (**$PT_2$BTDPPSB**). Aqueous tetra-*n*-butylammonium fluoride (TBAF), selected as base and solvent, proved crucial for maintaining solubility during the course of the polymerization. Estimated number-average molecular weight ($M_n$) values of the resulting polymers were 20–40 kDa (determined by size exclusion chromatography in 2,2,2-trifluoroethanol (TFE) relative to PMMA standards).[29] CPZs in this molecular-weight range give uniform films (average roughness of about 1 nm, according to atomic force microscopy (AFM) analysis following spin-casting onto the bulk heterojunction active layer; see Figure S1 in the Supporting Information). The resulting novel **$PT_3$SB** was designed to contain a similar density of SB side chains to that of **$PT_2$BTDPPSB** and **$PT_2$NDISB**, in an attempt to impart comparable CPZ–metal interactions for electrode work function modification across the different samples studied, while maintaining good solution processability. The DPP interlayer was chosen as a bench-mark, given its excellent performance as a cathode modification layer in PSCs relative to prior CPZs we have tested.[26,29] The novel **$PT_2$NDISB** was synthesized and incorporated into PSCs for comparison with the thiophene and DPP cases, potentially benefiting from the n-type electronic properties identified in alkyl-substituted NDI polymers.[30,31]

Optical energy gap ($E_g$) values were determined on thin CPZ films by their absorption onset (Figure S2), noting that **$PT_3$SB** had the largest $E_g$ (1.91 eV, red), **$PT_2$BTDPPSB** the smallest $E_g$ (1.22 eV, green), while **$PT_2$NDISB** was intermediate between ($E_g = 1.58$ eV, blue; Figure 1). Ionization potential ($I_P$) values were determined by ultraviolet photoelectron spectroscopy (UPS) from the low binding energy onset, with electron affinity ($E_A$) taken as the difference between $I_P$ and $E_g$. The higher $I_P$ (5.46 eV) and $E_A$ (3.88 eV) values for **$PT_2$NDISB** suggest hole-blocking and electron-extracting capabilities, respectively, relative to **$PT_3$SB** and **$PT_2$BTDPPSB**. For an interlayer that bridges the active layer and cathode, a large $E_A$ minimizes the barrier to electron transport from the active layer to the interlayer, which in turn minimizes $R_s$.

OPV devices were fabricated in a bulk heterojunction device architecture, using the narrow energy gap donor polymer, poly(benzodithiophene-*a*-thieno[3,4-*b*]thiophene) with 2-(ethylhexyl)thienyl side chains (PBDTT-TT), purchased from 1-Material Inc., and [6,6]-phenyl $C_{71}$-butyric acid methyl ester ($PC_{71}BM$) as the acceptor (Figure S3). An ITO/PEDOT:PSS/PBDTT-TT:$PC_{71}$BM/**CPZ**/Ag architecture was used for all fabricated PSCs. The CPZ was placed between the active layer and top reflective Ag cathode, selecting Ag in place of the more commonly used Al to highlight the utility of stable high-work-function metal electrodes in conjunction with CPZ interlayers. Figure 2a shows *J*–*V* curves for OPV devices containing no interlayer (bare Ag control) and **$PT_3$SB** (ca. 5 nm), **$PT_2$BTDPPSB** (ca. 8 nm), and **$PT_2$NDISB** (ca. 5 nm) interlayers of optimal thickness. The bare Ag devices gave a maximum PCE of 3.17%, while incorporation of **$PT_3$SB**, **$PT_2$BTDPPSB,** and **$PT_2$NDISB** interlayers improved PCE to average/maximum values of 5.08/5.09%, 9.39/9.49%, and 9.94/10.19%, respectively (averages calculated over six device measurements; Tables S1–S3). This markedly improved device performance stems from the substantial increase in $V_{OC}$ (ca. 0.44 to 0.75 V) and *FF* (ca. 42 to 70%), as well as $J_{SC}$ (ca. 17.5 to 19 mA cm$^{-2}$) and reduced $R_s$ (ca. 9.5 to 3.5 Ω cm$^2$) for **$PT_2$NDISB**.

The effect of CPZ interlayer thickness on device performance was investigated by varying CPZ concentration for spin coating, yielding thicknesses from nominally 1 nm up to > 20 nm (Figure 2b, Figure S4, and Tables S1–S3). The performance of OPVs containing **$PT_3$SB** was sensitive to interlayer thickness, with appreciable reduction in PCE noted for layers exceeding 5 nm because of a large decrease in *FF* and $J_{SC}$ and increased $R_s$ (Table S1–S3). In contrast, both **$PT_2$DPPSB** and **$PT_2$NDISB** proved more tolerant to variation in interlayer thickness, with $V_{OC}$ (0.75 V), *FF* (70%) and $R_s$ (3.5 Ω cm$^2$) plateauing at 5–10 nm thickness, but maintaining near maximum values at > 20 nm thickness. In addition, $J_{SC}$ was not significantly influenced by the CPZ interlayer thickness, with values exceeding 16 mA cm$^{-2}$ across the entire thickness range investigated for **$PT_2$DPPSB** and **$PT_2$NDISB**.

The electronics of CPZ films were studied by UPS to determine their interaction with Ag (Figure 3a), and by space charge limited current (SCLC) measurements to estimate

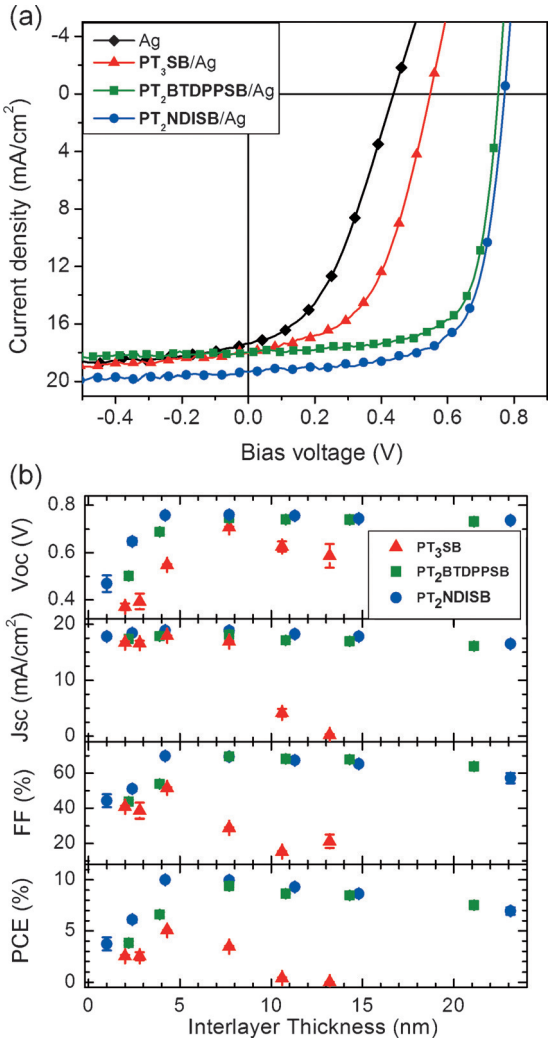


***Figure 2.*** Solar-cell performance of OPV devices with the architecture and composition of ITO/PEDOT:PSS/PBDTT-TT:$PC_{71}BM$/**(CPZ)**/Ag. a) *J–V* curves for OPV devices containing no interlayer (bare Ag) and **$PT_3SB$**, **$PT_2BTDPPSB$,** and **$PT_2NDISB$** cathode modification layers. b) OPV device metrics as a function of interlayer thickness (±1 standard deviation for each point was obtained from more than six devices).

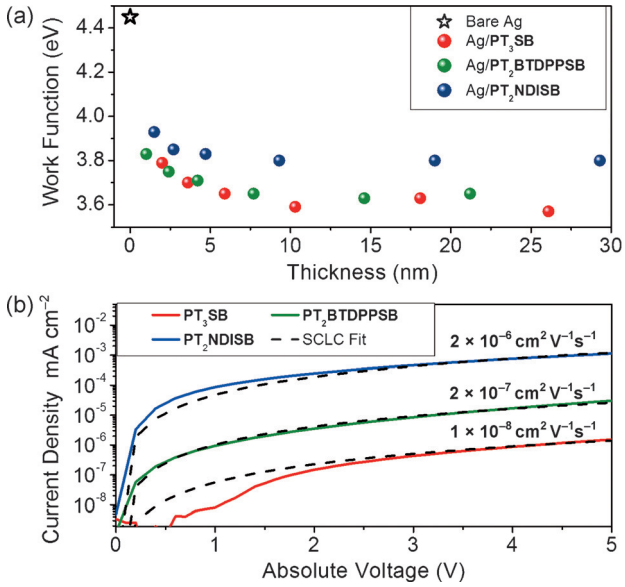


***Figure 3.*** Electronic characterization of CPZ films. a) Effect of CPZ thickness on the work function of Ag; b) Relative electron mobilities of CPZs estimated using the Mott–Gurney law in SCLC regime for device architecture ITO/CPZ/Ca/Al.

electron mobility (Figure 3b). By UPS, the secondary electron cutoff ($E_{SEC}$) in the high binding energy region probes the effect of CPZs on the work function of Ag, where the difference in $E_{SEC}$ for bare Ag and CPZ-coated Ag yields $\Delta$ values. Ultrathin (<2 nm) CPZ layers led to an $\Delta$ ranging from −0.5 to −0.6 eV, corresponding to a reduction in work function from 4.45 eV (native Ag) to 3.9 eV. Increasing the CPZ layer thickness led to further work function reduction to 3.8 eV for **$PT_2NDISB$** and 3.6 eV for **$PT_3SB$** and **$PT_2BTDPPSB$** (Figure 3a), a finding attributed to better film uniformity and fewer pinholes.[26] Interlayer thickness tracked closely with $V_{OC}$ values in the PSCs, with peak performance at about 8 nm interlayer thickness that remained nearly constant with increasing thickness.

To better understand these findings, electron only devices with an architecture of ITO/CPZ/Ca/Al were fabricated to estimate electron mobility using SCLC and fitting with the Mott–Gurney law, finding $1\times10^{-8}\,cm^2\,V^{-1}\,s^{-1}$ for **$PT_3SB$**, $2\times10^{-7}\,cm^2\,V^{-1}\,s^{-1}$ for **$PT_2BTDPPSB$,** and $2\times10^{-6}\,cm^2\,V^{-1}\,s^{-1}$ for **$PT_2NDISB$** (Figure 3b). These values were obtained using dielectric constants ($\varepsilon$) of about 5, determined separately by impedance spectroscopy (Figure S5). The higher electron mobility of **$PT_2BTDPPSB$** and **$PT_2NDISB$** explain their superior performance with increasing interlayer thickness, as these interlayers are less prone to charge accumulation at the active-layer/CPZ interface which would lead to increased $R_s$ and reduced *FF* and $J_{SC}$ (Figure 2b). The small $E_A$ for **$PT_3SB$** may contribute to its inferior performance relative to the other polymers. For **$PT_2BTDPPSB$** and **$PT_2NDISB$**, the relatively constant *FF* for devices with interlayer thickness exceeding 5 nm suggests that electron transport is not significantly impeded in these thicker layers, irrespective of their difference in electron mobility.

Optical characterization of the PSCs distinguished interlayer and active layer absorption, providing insight into the origin of $J_{SC}$ enhancement. Reflectance spectroscopy performed on OPV devices containing a 4–8 nm CPZ interlayer were compared to devices with no interlayer. This revealed a 4% decrease in reflectance from 650–700 nm, corresponding to enhanced absorption over those wavelengths for devices containing CPZ interlayers (Figures S6 and S7). External quantum efficiency (EQE) measurements show larger photocurrent collection in the active layer absorption regime (600–740 nm) for devices containing CPZ interlayers relative to devices with no interlayer (bare Ag control), corresponding to larger $J_{SC}$ (Figure 4). Absorption from the CPZ interlayers (Figure S2) cannot account for the observed changes in reflectance spectra or EQE. Thus, the CPZs are considered as optical spacers that redistribute the optical field within the device and enhance active layer absorption.[32]

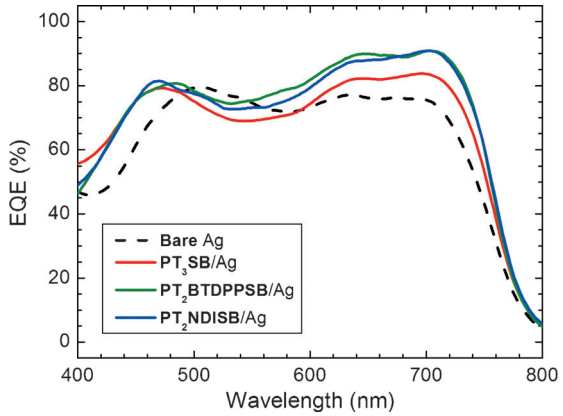


***Figure 4.*** External quantum efficiency (EQE) spectra of optimized OPV devices containing CPZ interlayers versus devices having no interlayer.

In summary, new CPZs were synthesized and incorporated into PSCs as cathode modification layers, enhancing optimized PCE values from 3.17% for devices containing no interfacial layer (bare Ag cathode) to 5.09%, 9.49%, and 10.19% for devices containing **$PT_3SB$**, **$PT_2BTDPPSB$**, and **$PT_2NDISB$** interlayers, respectively. The dramatic improvement in device performance for the DPP and NDI-based interlayers stems from a combination of their ability to effectively lower the work function of the metal cathode, increase the built-in electrostatic device potential, and maintain a low $R_s$ because of more efficient electron transport across the interlayer. The CPZs act as optical spacers to enhance total photocurrent generated within the active layer. The less efficient electron transport properties of **$PT_3SB$** leads to interfacial charge build-up and lower PCE values, while both **$PT_2DPPSB$** and **$PT_2NDISB$** maintain high PCE values for interlayer thickness exceeding 20 nm, because of their higher intrinsic electron mobilities. In particular, the NDI-based CPZ interlayers led to very high efficiencies, even exceeding 10% PCE. More importantly, the structure–property relationships uncovered in this work provide guidelines for future development of functional interfaces and interlayers towards further enhancement of polymer-based solar-cell technology.

## Acknowledgements

This research was supported by the Polymer Based Materials for Harvesting Solar Energy (PHaSE), an Energy Frontier Research Center funded by the U.S. Department of Energy (DOE) Office of Basic Energy Sciences, under award DE-SC0001087, and the National Science Foundation (grant number NSF-CHE 1152360) for polymer-functionalized surfaces and interfaces. PHaSE and the UMass MRSEC on Polymers (DMR-0820506) are acknowledged for facilities support. Volodimyr V. Duzhko assisted with impedance spectroscopy measurements, and we thank Alyson Grigoli for designing the TOC graphic artwork.

**Keywords:** dipoles · interfacial layers · polymers · power conversion efficiency · solar cells

**How to cite:** *Angew. Chem. Int. Ed.* **2015**, *54*, 11485–11489
*Angew. Chem.* **2015**, *127*, 11647–11651

[1] H.-L. Yip, A. K.-Y. Jen, *Energy Environ. Sci.* **2012**, *5*, 5994.
[2] Z. He, H. Wu, Y. Cao, *Adv. Mater.* **2014**, *26*, 1006.
[3] Z. He, C. Zhong, S. Su, M. Xu, H. Wu, Y. Cao, *Nat. Photonics* **2012**, *6*, 591.
[4] K. Yao, M. Salvador, C. Chueh, X. Xin, Y. Xu, W. Dane, T. Hu, Y. Chen, D. S. Ginger, A. K. Jen, *Adv. Energy Mater.* **2014**, *4*, 1400206.
[5] W. Zhang, Y. Wu, Q. Bao, F. Gao, J. Fang, *Adv. Energy Mater.* **2014**, *4*, 1400359.
[6] X. Guo, M. Zhang, W. Ma, L. Ye, S. Zhang, S. Liu, H. Ade, F. Huang, J. Hou, *Adv. Mater.* **2014**, *26*, 4043.
[7] C.-Z. Li, C.-Y. Chang, Y. Zang, H.-X. Ju, C.-C. Chueh, P.-W. Liang, N. Cho, D. S. Ginger, A. K.-Y. Jen, *Adv. Mater.* **2014**, DOI: 10.1002/adma.201402276.
[8] Z. a. Page, Y. Liu, V. V. Duzhko, T. P. Russell, T. Emrick, *Science* **2014**, *346*, 441.
[9] K. M. O'Malley, C.-Z. Li, H.-L. Yip, A. K.-Y. Jen, *Adv. Energy Mater.* **2012**, *2*, 82.
[10] X. Yang, C. Chueh, C. Li, H. Yip, P. Yin, H. Chen, W. Chen, A. K. Jen, *Adv. Energy Mater.* **2013**, *3*, 666.
[11] C. Chueh, S. Chien, H. Yip, J. F. Salinas, C. Li, K. Chen, F. Chen, W. Chen, A. K. Jen, *Adv. Energy Mater.* **2013**, *3*, 417.
[12] Q. Mei, C. Li, X. Gong, H. Lu, E. Jin, C. Du, Z. Lu, L. Jiang, X. Meng, C. Wang, Z. Bo, *ACS Appl. Mater. Interfaces* **2013**, *5*, 8076.
[13] S. Li, M. Lei, M. Lv, S. E. Watkins, Z. Tan, J. Zhu, J. Hou, X. Chen, Y. Li, *Adv. Energy Mater.* **2013**, *3*, 1569.
[14] Y.-Y. Lai, P.-I. Shih, Y.-P. Li, C.-E. Tsai, J.-S. Wu, Y.-J. Cheng, C.-S. Hsu, *ACS Appl. Mater. Interfaces* **2013**, *5*, 5122.
[15] X. Li, W. Zhang, Y. Wu, C. Min, J. Fang, *J. Mater. Chem.* **2013**, *1*, 12413.
[16] C. Duan, C. Zhong, C. Liu, F. Huang, Y. Cao, *Chem. Mater.* **2012**, *24*, 1682.
[17] Z.-G. Zhang, B. Qi, Z. Jin, D. Chi, Z. Qi, Y. Li, J. Wang, *Energy Environ. Sci.* **2014**, *7*, 1966.
[18] Y. Zhou, C. Fuentes-Hernandez, J. Shim, J. Meyer, A. J. Giordano, H. Li, P. Winget, T. Papadopoulos, H. Cheun, J. Kim, M. Fenoll, A. Dindar, W. Haske, E. Najafabadi, T. M. Khan, H. Sojoudi, S. Barlow, S. Graham, J.-L. Brédas, S. R. Marder, A. Kahn, B. Kippelen, *Science* **2012**, *336*, 327.
[19] S. Woo, W. Hyun Kim, H. Kim, Y. Yi, H.-K. Lyu, Y. Kim, *Adv. Energy Mater.* **2014**, *4*, 1301692.
[20] C. Gu, Y. Chen, Z. Zhang, S. Xue, S. Sun, C. Zhong, H. Zhang, Y. Lv, F. Li, F. Huang, Y. Ma, *Adv. Energy Mater.* **2014**, *4*, 1301771.
[21] B. J. Worfolk, T. C. Hauger, K. D. Harris, D. A. Rider, J. A. M. Fordyce, S. Beaupré, M. Leclerc, J. M. Buriak, *Adv. Energy Mater.* **2012**, *2*, 361.
[22] Z. He, C. Zhong, X. Huang, W. Wong, H. Wu, L. Chen, S. Su, Y. Cao, *Adv. Mater.* **2011**, *23*, 4636.
[23] J. H. Seo, A. Gutacker, Y. Sun, H. Wu, F. Huang, Y. Cao, U. Scherf, A. J. Heeger, G. C. Bazan, *J. Am. Chem. Soc.* **2011**, *133*, 8416.
[24] J. Jo, J.-R. Pouliot, D. Wynands, S. D. Collins, J. Y. Kim, T. L. Nguyen, H. Y. Woo, Y. Sun, M. Leclerc, A. J. Heeger, *Adv. Mater.* **2013**, *25*, 4783.
[25] R. Kang, S. Oh, D. Kim, *ACS Appl. Mater. Interfaces* **2014**, *6*, 6227.
[26] F. Liu, Z. Page, V. Duzhko, T. P. Russell, T. Emrick, *Adv. Mater.* **2013**, *25*, 6868.
[27] C. Duan, K. Zhang, X. Guan, C. Zhong, H. Xie, F. Huang, J. Chen, J. Peng, Y. Cao, *Chem. Sci.* **2013**, *4*, 1298.

[28] Z. A. Page, F. Liu, T. P. Russell, T. Emrick, *Chem. Sci.* **2014**, *5*, 2368.
[29] Z. A. Page, F. Liu, T. P. Russell, T. Emrick, *J. Polym. Sci. Part A* **2015**, *53*, 327.
[30] H. Yan, Z. Chen, Y. Zheng, C. Newman, J. R. Quinn, F. Dötz, M. Kastler, A. Facchetti, *Nature* **2009**, *457*, 679.
[31] Y.-J. Hwang, T. Earmme, B. A. E. Courtright, F. N. Eberle, S. A. Jenekhe, *J. Am. Chem. Soc.* **2015**, *137*, 4424.
[32] J. Y. Kim, S. H. Kim, H.-H. Lee, K. Lee, W. Ma, X. Gong, a. J. Heeger, *Adv. Mater.* **2006**, *18*, 572.

Received: April 29, 2015
Published online: July 31, 2015

  